Article

Investigation of Diffusible Hydrogen Concentration in Gas Metal Arc Brazing by Carrier Gas Hot Extraction Method Referring to ISO 3690

Oliver Brätz [1,*], Benjamin Ripsch [1], Andreas Gericke [1] and Knuth-Michael Henkel [1,2]

1   Fraunhofer Institute for Large Structures in Production Engineering IGP, 18059 Rostock, Germany
2   Faculty of Mechanical Engineering and Marine Technologies, Joining Technology, University of Rostock, 18059 Rostock, Germany
*   Correspondence: oliver.braetz@igp.fraunhofer.de; Tel.: +49-381-49682-231

Abstract: Arc brazing is an alternative joining technology well-suited for processing thermally sensitive materials and to produce mixed material connections. Due to the technological similarities of gas metal arc brazing to gas metal arc welding, it can be assumed that the process-related hydrogen input is of similar magnitude for both joining technologies. Since diffusible hydrogen is known to cause embrittlement in metallic materials, it is necessary to know the amount of diffusible hydrogen introduced by different manufacturing processes. Regarding the qualification of welding procedures, hydrogen ingress is an important factor to evaluate the risk of hydrogen-assisted cold cracking, especially when processing high-strength steels. For arc brazing, there is a lack of knowledge about the process-related hydrogen input. Hence, to study the influence of different brazing filler materials and varying levels of heat input on the diffusible hydrogen concentration in arc braze metal, a methodology to determine hydrogen content in arc weld metal in accordance with international standard ISO 3690 based on carrier gas hot extraction was applied to arc brazed specimens. Very low diffusible hydrogen concentrations of about H_D = 0.1 to 0.3 mL/100 g were found for GMAB without significant influence of arc energy or filler metal used.

Keywords: hydrogen-assisted cold cracking HACC; copper; bronze; MSG soldering; braze welding; hydrogen analysis; thermal desorption analysis TDA

1. Introduction

Gas metal arc brazing (GMAB), also referred to as arc brazing, is a modification of the gas metal arc welding (GMAW) process. In contrast to GMAW, a filler material with a considerably lower melting point compared to the base material's melting point is used for GMAB. Other than that, the same GMAW equipment is used for GMAB. Referring to the process temperature, arc brazing belongs to the category of high-temperature brazing processes (process number 973 according to ISO 4063 [1]). Due to the low melting temperatures of the brazing materials, i.e., usually copper–silicon and copper–aluminium alloys, arc brazing has a lower thermal impact on the base material compared to arc welding. The arc is used as heat source for cleaning or activating the surface and for melting the filler material. In contrast to welding, melting of the parent material is generally not intended in arc brazing but usually ocurs to a small extent, cf. Figure 1a. The bonding mechanism is determined by interfacial reactions in the diffusion zone. An ultimate tensile strength of up to 700 MPa can be reached by arc brazed connections. Pure argon or helium are generally used as shielding gases, sometimes with low doping of active components [2]. In the automotive industry, arc brazing is an established joining process for thin galvanized sheet metal (thickness $t \leq 3$ mm) [2–4]. In contrast, in steel construction ($t > 3$ mm), arc brazing is not currently a common joining process. However, due to benefits in terms of heat input and fatigue strength of arc brazed joints compared to welded connections, different fields

of application are starting to emerge in steel construction as well [5,6]. For instance, fatigue strength benefits of steel plates with arc brazed attachments rather than welded joints will be acknowledged in shipbuilding rules by implementing the use of arc brazing as an alternative joining process for fatigue life improvement in the upcoming revision of DNV's class guideline DNV-CG-0129 "Fatigue assessment of ship structures" [7]. In addition, arc brazing is used to join socket connections of piping sections due to minimization of damage to the galvanized pipes, cf. Figure 1b.
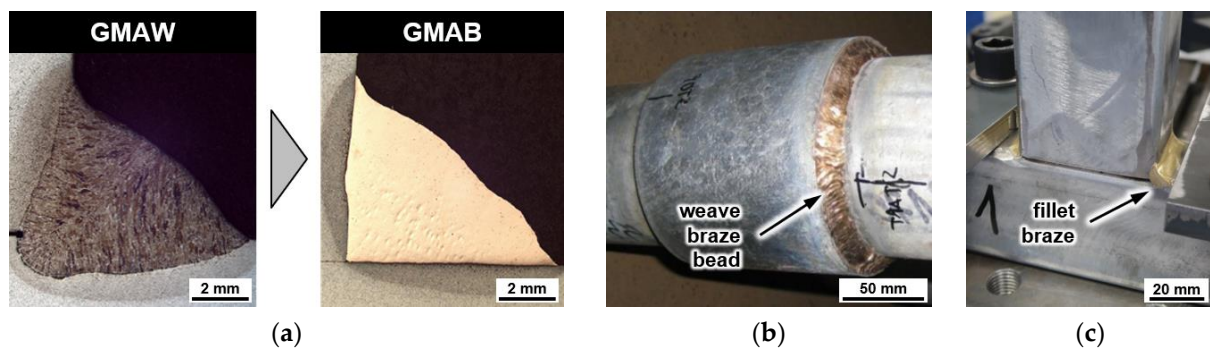
Figure 1. Application of arc brazing: (**a**) comparison of fillet welded and fillet brazed joint; (**b**) arc brazed grey water pipe socket in ship building; (**c**) arc brazed hollow section T-joint in steel construction. (© Fraunhofer IGP).

A major issue in the arc welding of steels is the risk of hydrogen assisted cold cracking (HACC), especially for high-strength grades [8–10]. Hydrogen is known to effect material embrittlement and in case of reaching a critical state of susceptible microstructure, local mechanical stresses and sufficient local concentrations of diffusible hydrogen HACC occurs. The complex mechanisms of hydrogen-induced embrittlement of metals are widely discussed and described by different theories, cf. [8,11]. For welded structures, HACC is particularly critical due the delayed occurrence of potentially catastrophic failures [8,12]. In recent studies, different methods for reducing the diffusible hydrogen content in deposited metal were investigated, with a focus on reducing the risk of HACC for high-strength steels. Welding procedure modification and adjusting the bevel configuration are promising in this regard [12–14].

The hydrogen input in arc welding is a result of the presence of hydrogen in the arc atmosphere, hydrogen contaminated filler material or local hydrogenous residues on parent material. During welding, molecolar hydrogen is dissociated by the arc energy and is then easily absorbed by the molten material. The grain-coarsened region of the heat-affected zone (GCHAZ) is usually characterized by a hardened microstucture with reduced ductility due to the quenching effect upon welding. Combined with the proximity of the GCHAZ to the weld bead and the higher solubility of hydrogen in austenite, this region is particularly susceptible for HACC, cf. [8,15].

For arc brazing, the mechanism for hydrogen input and diffusion is assumed to be equivalent to GMAW. Although a very low hydrogen solubility is generally expected for copper alloys [16], extensive hydrogen trapping may occur in all technical alloys due to material defects [17]. Therefore, copper-based alloys only exhibit low suceptibility to hydrogen embrittlement, but due to higher diffusivity of hydrogen in copper than in austenite [18] and the thermally induced phase transformations in the steel base material heat-affected zone (HAZ), assessing the risk of hydrogen embrittlement is of interest for GMAB as well. Thus, the determination of the diffusible hydrogen concentration in arc brazed metal is essential to evaluate the risk of HACC. Until now, the diffusible hydrogen content in GMAB beads has not been investigated. For this reason, first investigations on the influence of different brazing filler materials and varying levels of heat input on the diffusible hydrogen concentration in arc braze metal were carried out and are presented in this study.

2. Hydrogen Analysis

The determination of hydrogen contents caused by welding can be carried out by means of various quantitative elemental analysis methods. All test methods involve welding under defined conditions followed immediately by deep-freezing of the test specimens as fast as possible. This way, unwanted diffusion and effusion processes are inhibited and the hydrogen introduced to the weld metal is conserved. Subsequently, the diffusible hydrogen is desorbed from the test specimens in a controlled manner. Different temperature ranges and aging times are defined for the outgassing. Methods without thermally assisted effusion, such as the mercury method, require aging times of several days to ensure complete outgassing of the specimens. Thermodesorption methods allow lower minimum extraction times of well below 1 h, depending on temperature, and give values at least as accurate as effusion methods without heat supply [19]. The detection of the extracted hydrogen volume can be performed simultaneously to the desorption by means of carrier gas hot extraction analysis (CGHE) [20] in vacuum or decoupled by means of various metrological methods for quantitative gas analysis. Typical current gas chromatographic measurement methods used for quantitative hydrogen analysis include thermal conductivity detectors (TCDs), mass spectrometers, or fluid column eudiometers (mercury, silicone oil). Older practices using glycerin for hydrogen evolution are no longer recommended due to identified systematic inaccuracies of these methods [21]. In addition to the diffusible hydrogen content, the total hydrogen content (including residual fraction and hydrides) can be determined by high thermal activation or melting of the specimens. Since the residual hydrogen is not relevant with respect to possible HACC phenomena, it will not be discussed further.

As an international standard for the determination of the diffusible hydrogen content in the arc weld metal of martensitic, bainitic and ferritic steels, ISO 3690 defines the procedure for the production of specimens as well as their cleaning, storage, and analysis [21]. The methods of analysis specified are the measurement of mercury displacement and TCD method by CGHE, which is currently the most widely applied method due to its high precision and relatively fast testing procedure.

The characteristic hydrogen contents are typically given for the deposit weld metal as H_D in mL/100 g or for the total weld metal mass H_F in ppm. The hydrogen content or concentration is given for the weld metal, although the diffusible hydrogen is distributed over weld metal and HAZ in particular, depending on the welding procedure (process and weld configuration) [8,22] and the material welded [23,24].

The hydrogen concentrations present in the arc weld metal are multifactorially dependent on the welding procedure (process and parameters [25,26]), the consumables used, as well as the environmental conditions (e.g., humidity). In addition, the thermal field present determines the hydrogen concentration immediately after welding [26,27]. For GMAW, a relatively low hydrogen input of about H_D = 1 to 4 mL/100 g can be expected when welding under typical workshop conditions, cf. [19]. For qualitative assessment, a hydrogen content of more than 15 mL/100 g is considered high and a hydrogen content of less than 5 mL/100 g is considered very low. However, for sensitive microstructures of high-strength materials, contents of around 2 mL/100 g can already be critical with regard to the occurrence of HACC [12,23].

So far, the diffusible hydrogen content in arc braze metal has not been examined.

3. Materials and Methods

3.1. Sample Preparation

Specimens for hydrogen analysis were generally produced in accordance with ISO 3690 [21]. However, instead of arc welding, GMAB was applied. Two different kinds of copper-based filler metals were used to produce different series of arc brazed deposit beads on steel plates. For each series, three specimens using the same consumables and brazing parameters were produced. CuSi3Mn1 ($R_m \approx 350$ MPa, $A \approx 40\%$) and CuAl7 ($R_m \approx 430$ MPa, $A \approx 40\%$) according to ISO 24373 [28] with a diameter of 1.0 mm were

used as solid wire brazing electrodes [5]. As required by ISO 3690 [21], non-alloyed plain carbon steel in a degassed condition (650 °C for 1 h) was used as base material (1.0570 according to EN 10027-2 [29]). The chemical composition of base and filler material was verified by optical emission spectrometry (OES) using a spark spectrometer (Spectromaxx, Spectro Analytical Instruments GmbH), cf. Table 1.

Table 1. Chemical compositions of used materials, in wt%.

Material		Cu	Al	Fe	Mn	Ni + Co	P	Pb	Si	Sn	Zn
filler 1 CuSi3Mn1	$\bar{x}$ (n = 3) (s_x)	95.95 (0.04)	<0.0010 (0.0003)	0.062 (0.008)	0.82 (0.01)	0.013 (0.001)	0.0078 (0.0003)	<0.0010 (0.0005)	2.91 (0.05)	0.0040 (0.0000)	<0.0015 (0.0005)
filler 2 CuAl7	$\bar{x}$ (n = 3) (s_x)	85.68 (0.20)	7.73 (0.07)	2.14 (0.07)	1.43 (0.04)	2.42 (0.02)	0.018 (0.001)	0.029 (0.004)	0.050 (0.022)	0.0074 (0.0009)	<0.0015 (0.0019)
		C	Si	Mn	Cr	Mo	V	Ni	Cu	Al	Fe
base metal 1.0570	$\bar{x}$ (n = 10) (s_x)	0.065 (0.0075)	0.311 (0.012)	1.36 (0.013)	0.022 (0.0003)	<0.0010 (0.0002)	<0.0010 (0.0002)	0.0138 (0.0003)	0.013 (0.0045)	0.048 (0.0005)	98.08 (0.023)

A gas metal arc welding machine (S5 SpeedPulse XT, Lorch Schweißtechnik GmbH) was used for arc brazing. For guiding the welding torch and to ensure reproducible brazing results, constant heat input and constant quality of the arc brazed beads, a collaborative robot (UR10, Universal Robots GmbH) was used. For each brazing consumable, sets of specimens were produced with high and low heat input or high and low arc energy, respectively. Brazing parameters were measured (WeldAnalyst S3, HKS Prozesstechnik GmbH, f_s = 10 kHz) as summarized in Table 2.

Table 2. Arc brazing parameters.

Sample/Series	Polarity	Voltage [1] U in V	Current [1] I in A	Brazing Speed v in m/min	Arc Energy [2] E in kJ/mm
A: CuSi3Mn1 high energy	~AC	30.6	204	0.45	0.83
B: CuSi3Mn1 low energy	~AC	27.6	158	0.45	0.58
C: CuAl7 high energy	~AC	32.0	195	0.45	0.83
D: CuAl7 low energy	~AC	30.5	144	0.45	0.58

[1] Root mean square/effective value. [2] Arc Energy as heat input acc. to ISO/TR 17671-1 neglecting the thermal efficiency factor.

The manufacturing setup, the specimen geometry, and a microsection of a brazed bead are shown in Figure 2. Arc brazed deposit beads were brazed onto a three-piece steel plate clamped in a copper fixture. The geometry of assembly type A according to ISO 3690 was chosen, cf. Figure 2b. The test piece assembly was cleaned in acetone and weighed prior to being clamped. Additionally, annealed copper foil strips (t = 1 mm) were used to facilitate thermal transfer. During GMAB, typical atmospheric workshop conditions were present, with a room temperature of T = 25 ± 2 °C and a relative humidity of φ = 60 ± 10%. After extinction of the arc, the test piece assembly was removed from the fixture and subsequently (4 ± 1 s) immersed in an ice water bath; then, after 20 s, the specimens were transferred to another container and completely immersed in a bath of liquid nitrogen (−196 °C) for freezing. After a minimum of 5 min, the test assembly was taken out for cleaning from slag and welding fume residues by steel wire brushing. Then, the run-on and run-off pieces were broken off from the relevant center test piece. By doing so, it was assured that time outside of the liquid nitrogen bath did not exceed 60 s. After each cleaning step, the center test piece was returned to the low temperature bath for a minimum of 2 min before progressing. Finally, the center piece was stored in a silicon oil bath (−80 °C) for less than 72 h before CGHE analysis.
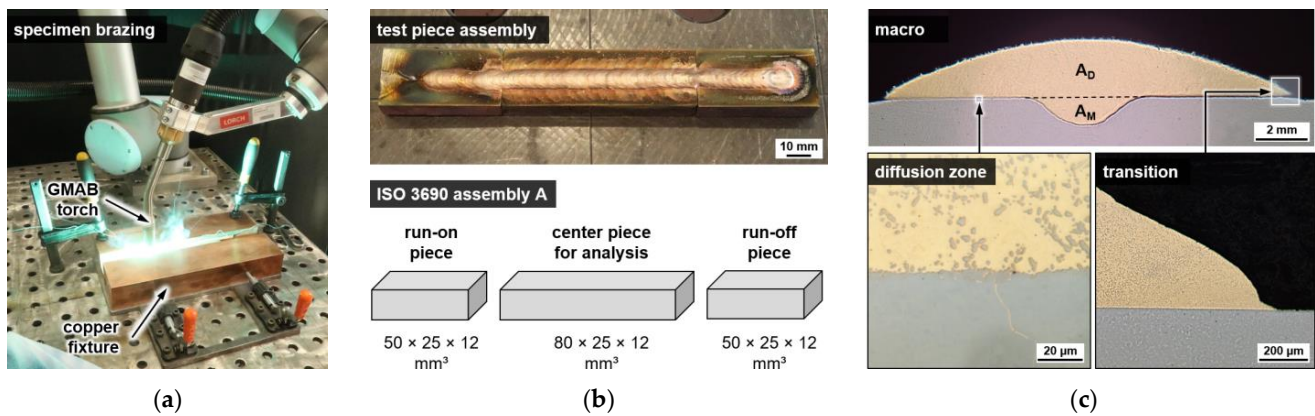
Figure 2. Production of specimens, (**a**) arc brazing of test piece assembly, (**b**) test piece for hydrogen analysis and (**c**) cross section of the test piece.

3.2. Measurement of Hydrogen

The diffusible hydrogen was measured using the CGHE method. To determine the thermally desorbed hydrogen volumes, a gas analysis system with an external infrared (IR)-furnace (G8 Galileo + IR-07, Bruker Corporation) was used, cf. Figure 3a. The analyzer is equipped with two serially arranged TCDs to cover a particularly wide range. High purity nitrogen ISO 14175-N1 ($N_2 \geq 99.999$ vol.%) was used as inert carrier gas. The carrier gas was first fed to the external IR-furnace in which the thermodesorption of the test specimen's diffusible hydrogen takes place. For the hydrogen extraction, the specimens were heated to 400 °C and kept for a dwell time of 0.35 h (1260 s) as required in the ISO 3690 [21]. In the furnace glass tube, effused H_2, CO, and possibly H_2O of the radiation-heated specimen were added to the analysis stream. After selective purification, the binary analysis gas was analysed by means of TCD. A prior calibration of the TCDs was done by the internal gas calibration device using high purity helium ISO 14175-I2 (He $\geq$ 99.996 vol.%) During the measurement, the temperature of the IR-furnace was recorded via an external thermocouple and the signal of the TCDs representing the H_2 effusion rate was recorded at a frequency of f_s = 5 Hz. The effused hydrogen volume under standard temperature and pressure V_{STP} was determined by integrating the TCD signal in the region of the peak above the baseline. The interval limits were set automatically and corrected manually, cf. Figure 3b.
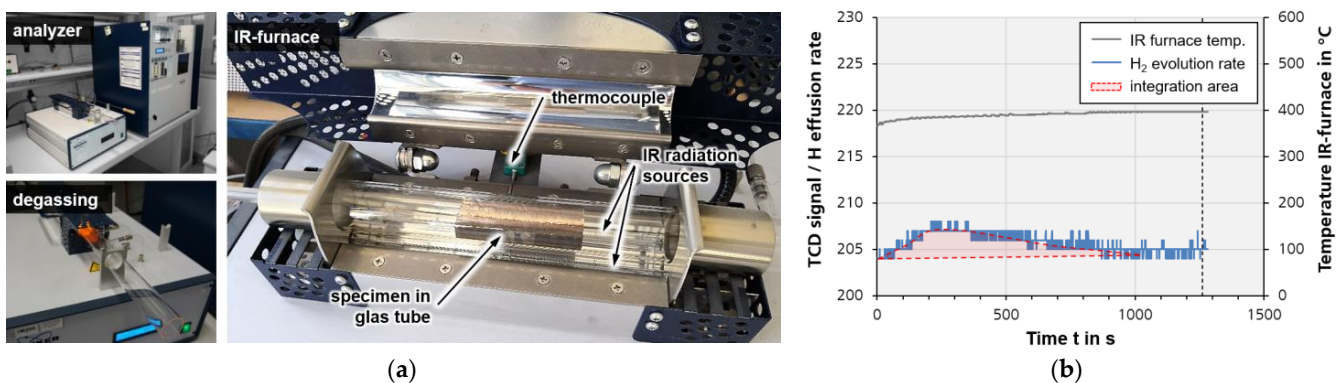
Figure 3. Measurement of hydrogen by carrier gas hot extraction using thermal conductivity detector method; (**a**) test specimen in IR-furnace for degassing; (**b**) signal course during thermal desorption analysis.

To determine the hydrogen concentration, the measured hydrogen volume V_{STP} was related to specific masses. Analogous to deposit welding, the proportions of the deposited metal mass m_D and the total fused metal mass m_F, representing the sum of m_D and the molten base metal m_M, were determined. The mass of the deposited metal was calculated as difference of the mass of the center test piece after brazing and its initial mass, both

being weighed accordingly. Thus, the hydrogen content in the deposited metal H_D was calculated acc. to Equation (1) [21].

$$H_D = V_{STP} \cdot \frac{100}{m_D} \text{ (in mL/100 g)} \tag{1}$$

The average area of deposited braze metal A_D and the average area of fused metal A_F were determined at macro sections of the test pieces by using an image-analyzing microscope. The content of diffusible hydrogen in fused braze metal is calculated according to Equation (2) [21]. Due to the very low penetration and dilution in arc brazing, the influence of the base material's higher density is neglected.

$$H_F = H_D \cdot 0.9 \cdot \frac{A_D}{A_F} \text{ (in ppm)} \tag{2}$$

4. Results and Discussion

4.1. Metallography

Microsections were prepared according to ISO 17639 [30] from the hydrogen analysis samples after hydrogen analysis. Exemplarily, microsections of beads on plates of each filler metal used are shown below; see Figure 4. Typical for arc brazing processes, a fusion zone can be found in the middle of the bead at all micro sections prepared. This is the area where the brazing arc contacted and melted the base metal, enabling penetration and dilution of the base metal with the filler metal [31]. Correspondingly, the braze metal was characterized by a dense formation of mainly ferritic intermetallic compounds inside the copper-based matrix. With a generally higher content of alloy metals, segregation zones are visible around the intermetallic phases of CuAl7 braze metal, appearing in a brownish and darker tone than the surrounding copper when etched with Klemm's Reagent III (30 g potassium metabisulphite, 100 mL distilled water, and 11 mL stock solution: saturated aqueous sodium thiosulfate). In the base metal, the HAZ can be clearly separated from the areas not influenced by the heat of the brazing process, cf. microsections etched with Nital (3% nitric acid in ethanol) in Figure 4. In the centre of the bead, high heat dissipation led to formation of a GCHAZ with a martensitic/bainitic microstructure, whereas the HAZ at the transition region of the beads can be characterized as a fine-grained region (FGHAZ) and an intercritically heated region (ICHAZ), respectively.

Etched with Klemm's Reagent III, which renders ferritic compounds blue to brown, the diffusion zone can be distinctly distinguished from the surrounding material and is located at the braze metal/base metal interface. The diffusion zone is about 5 μm thin. Moreover, braze metal partly penetrates the base metal along its former austenite grain boundaries, known as intergranular liquid metal penetration (LMP), also a typical phenomenon in arc brazing processes [32,33].

The areas of deposited braze metal A_D and fused metal A_F measured are listed in Table 3. Depending on the process energy, different deposit rates and bead geometries were achieved. The procedures with higher arc energy led to an increase of the deposit metal area of about 60 to 70% and an increase of the size of the fusion zone of about 70 to 90%. Therefore, the high energy brazes tend to form more intermetallic compounds, caused by a higher degree of dilution compared to the low energy variants. Consequentially, the size of the HAZ is increased with higher arc energy. Exemplarily, one sample was prepared metallographically for each test series, and an increasement of the HAZ of about 100% was validated for the high heat input processes.
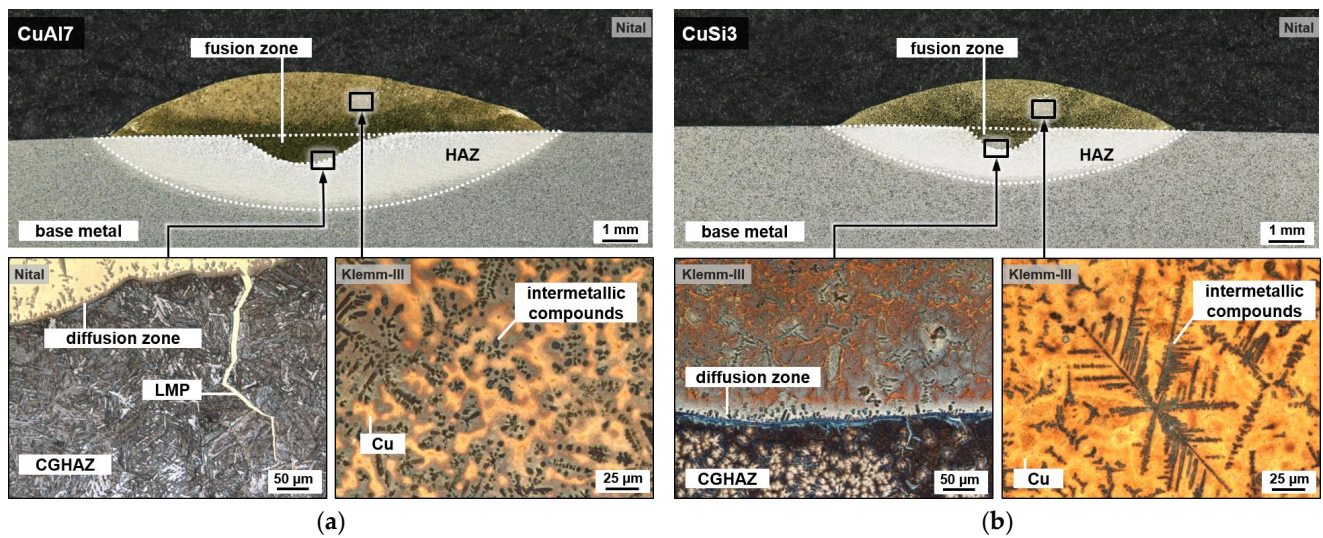
Figure 4. Microsection of an arc brazed bead on plate, etched with Nital 3% and Klemm-III; (**a**) CuAl7 filler, high heat input; (**b**) CuSi3 filler, low heat input.

Table 3. Bead geometry and hydrogen values.

Sample		Deposited Metal		Fused Metal		Diffusible Hydrogen		
		m_D in g	A_D in mm^2	A_F in mm^2	V_{STP} in mL	H_D in mL/100 g	H_F in ppm
A CuSi3Mn1 high energy	1	9.02	14.35	16.54	0.041	0.46	0.36
	2	9.29	15.35	17.40	0.011	0.12	0.09
	3	7.11	14.90	17.31	0.019	0.27	0.21
	$\overline{x}$	8.47	14.87	17.08	0.024	0.28	0.22
	(s_x)	(1.19)	(0.50)	(0.47)	(0.016)	(0.17)	(0.13)
B CuSi3Mn1 low energy	1	5.87	9.11	9.71	0.009	0.16	0.13
	2	6.04	9.57	10.51	0.004	0.06	0.05
	3	6.07	9.40	10.62	0.013	0.21	0.17
	$\overline{x}$	5.99	9.36	10.28	0.009	0.14	0.12
	(s_x)	(0.11)	(0.23)	(0.50)	(0.005)	(0.08)	(0.06)
C CuAl7 high energy	1	10.69	15.36	18.41	0.001	0.01	0.01
	2	9.91	15.12	18.14	0.009	0.09	0.07
	3	9.83	15.49	18.75	0.053	0.54	0.40
	$\overline{x}$	10.14	15.32	18.43	0.021	0.21	0.16
	(s_x)	(0.48)	(0.19)	(0.31)	(0.028)	(0.29)	(0.21)
D CuAl7 low energy	1	6.58	8.60	9.36	0.013	0.19	0.16
	2	6.14	9.33	9.56	0.042	0.68	0.59
	3	6.42	8.68	9.56	0.006	0.10	0.08
	$\overline{x}$	6.38	8.87	9.49	0.020	0.32	0.28
	(s_x)	(0.22)	(0.40)	(0.12)	(0.019)	(0.31)	(0.28)

4.2. Hydrogen Content

The mean values for the characteristic hydrogen concentrations H_D and H_F determined for the two filler metals and two levels of heat input are collectively illustrated in Figure 5. The error indicators represent the minimum and maximum values measured for each series.

Relatively low mean hydrogen concentrations in the range of about $H_D = 0.1$ to 0.3 mL/100 g were found for the deposited metal. A dependency on the used filler metal or the arc energy applied was not observed.
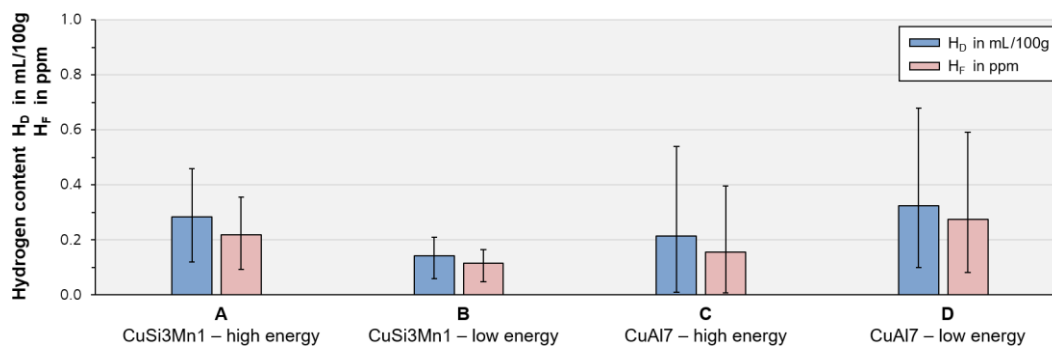
Figure 5. Hydrogen concentrations for GMAB using different filler metals and arc energies.

The hydrogen concentration in entire fused metal was determined to be in the range of about $H_F = 0.1$ to 0.3 ppm, as well. Generally, H_F values were found to be only a little lower than H_D values. For the high energy processes, H_F is approximately 75% of H_D, whereas for the low energy processes, H_F is only about 83% of H_D. This differs from typical welded beads, which usually show a significantly higher base metal penetration. For welded beads, H_F is typically about 50% of H_D, corresponding to a dilution of weld metal and base material of about 50% [21].

In general, very low hydrogen values were measured with high variances for all samples, cf. Table 3. Considering the variances of the results, no clear tendency regarding the influence of the process energy input on the resulting hydrogen concentration is noticeable, even though significantly higher deposit masses were analyzed.

Compared to conventional GMAW using steel wire consumables, the hydrogen concentrations found for arc brazed beads can be considered to be very low. For GMAW, diffusible hydrogen concentration H_D is usually in a range of about 1 to 4 mL/100 g, cf. [19]. The diffusible hydrogen content determined can be seen as technically neglectable, considering the typical reproducibility of hydrogen tests to be ± 1 mL/100 g, cf. [24], helium gas-calibrated TCD accuracy of about 0.1 ppm/g of specimen, and the general uncertainty of the CGHE method implying considerable relative standard deviations when analyzing low contents <1.5 mL/100 g, cf. [19,20]. In the investigations conducted, the TCD signal had comparatively small and relatively wide peaks, cf. Figure 3b. This kind of unfavorable signal form implies a low signal-to-noise ratio and impedes integrational evaluation of the data. Accordingly, the results show high variances, so an increased uncertainty in the results must be expected.

Moreover, for arc welding, it is proposed that a higher process energy, especially a higher arc length and welding voltage, leads to increased hydrogen ingress [26]. This could not be validated for GMAB. It is assumed that during arc brazing under conditions comparable to welding, equivalent hydrogen sources and intensities are available. The heat input of the process and subsequent cooling conditions are similar to welding as well. With the hydrogen input being expected to be of a similar magnitude for both kinds of joining processes, the solidified copper-based alloy seems to be able to trap the insoluble hydrogen energetically. Accordingly, the diffusible hydrogen content is very small, and the risk of HACC is therefore reduced. This means that, in addition to being beneficial for joining thermally sensitive materials and reducing stresses and distortion by applying a lower heat input, GMAB might also increase the joinability of HACC susceptible steels. Especially important for joining high-strength steels, a diffusible hydrogen concentration lower than 1 mL/100 g is, in some cases, essential to avoid cold cracking, cf. [10].

5. Conclusions and Outlook

The diffusible hydrogen content was investigated for arc brazing with different filler materials and heat input. For the determination of hydrogen concentrations, a methodology based on the rapid test method by CGHE using a TCD according to ISO 3690 was applied. The following findings were made:

I. The methodology for hydrogen determination in GMAW weld metal according to ISO 3690 can generally be applied for GMAB as well.
II. For arc brazed beads, low diffusible hydrogen concentrations in the range of $H_D = 0.1$ to 0.3 mL/100 g were found.
III. Due to characteristically low base metal penetration in GMAB compared to arc welding, the hydrogen concentration in the entire fused metal H_F is only about 5 to 18% lower than the corresponding hydrogen concentration in deposit metal.

Regarding the prevention of HACC in joining susceptible steels, GMAB might be a promising alternative to ordinary arc welding. The diffusible hydrogen concentrations in GMAB deposit metal were found to be only about one-tenth of the concentrations that can usually be found for GMAW or FCAW processes. Nonetheless, further investigations are necessary to study the mechanism of hydrogen diffusion and trapping in GMAB connections.

Abbreviations

CGHE	Carrier gas hot extraction
FCAW	Flux-cored arc welding
FGHAZ	Fine-grained heat-affected zone
GCHAZ	Grain-coarsened heat-affected zone
GMAB	Gas metal arc brazing
GMAW	Gas metal arc welding
HACC	Hydrogen-assisted cold cracking
HAZ	Heat-affected zone
ICHAZ	Intercritical heat-affected zone
LMP	Liquid metal penetration
MSG	Metal shielding gas (welding/brazing/soldering)
TCD	Thermal conductivity detector
TDA	thermal desorption analysis

References

1. *ISO 4063:2010-03*; Welding and Allied Processes–Nomenclature of Processes and Reference Numbers. International Organization for Standardization: Vernier, Geneva, Switzerland, 2010.
2. Pikuła, J.; Pfeifer, T.; Mendakiewicz, J. Influence of the shielding gas on the properties of VP MIG/MAG braze-welded joints in zinc coated steel sheets. *Bull. Inst. Weld.* **2014**, *1*, 35–41. [CrossRef]
3. Schwartz, M.M. *Brazing–Second Edition*; ASM International: Materials Park, OH, USA, 2003; ISBN 0-87170-784-5.
4. Nalajala, D.; Mookara, R.K.; Amirthalingam, M. Gas metal arc brazing behaviour of a galvanised advanced high strength steel in short circuiting and short circuiting with pulsing modes. *Weld. World* **2021**, *66*, 69–80. [CrossRef]
5. Andreazza, P.; Gericke, A.; Henkel, K.-M. Investigations on arc brazing for galvanized heavy steel plates in steel and shipbuilding. *Weld. World* **2021**, *65*, 1199–1210. [CrossRef]
6. Gericke, A.; Drebenstedt, K.; Kuhlmann, U.; Henkel, K. Improvement of fatigue strength in heavy steel constructions through arc brazing. *ce/papers* **2021**, *4*, 1118–1125. [CrossRef]
7. *DNV-CG-0129*; Class Guideline–Fatigue Assessment of Ship Structures. DNV AS: Bærum, Norway, 2021.

8. Bailey, N.; Coe, F.R.; Gooch, T.G.; Hart, P.H.M.; Jenkins, N.; Pargeter, R.J. *Welding Steels without Hydrogen Cracking*, 2nd ed.; Woodhead Publishing Limited: Cambridge, UK, 2004; ISBN 978-1-85573-014-6.

9. Lippold, J.C. *Welding Metallurgy and Weldability*; John Wiley & Sons, Inc.: Hoboken, NJ, USA, 2014; ISBN 978-1-11823-070-1.

10. Christ, M.; Guo, X.; Sharma, R.; Li, T.; Bleck, W.; Reisgen, U. Hydrogen Embrittlement Susceptibility of Gas Metal Arc Welded Joints from a High-Strength Low-Alloy Steel Grade S690QL. *Steel Res. Int.* **2020**, *91*, 2000131. [CrossRef]

11. Robertson, I.M.; Sofronis, P.; Nagao, A.; Martin, M.L.; Wang, S.; Gross, D.W.; Nygren, K.E. Hydrogen Embrittlement Understood. *Met. Mater. Trans. B* **2015**, *46*, 1085–1103. [CrossRef]

12. Wilhelm, E.; Mente, T.; Rhode, M. Waiting time before NDT of welded offshore steel grades under consideration of delayed hydrogen-assisted cracking. *Weld. World* **2021**, *65*, 947–959. [CrossRef]

13. Schaupp, T.; Schroeder, N.; Schroepfer, D.; Kannengiesser, T. Hydrogen-Assisted Cracking in GMA Welding of High-Strength Structural Steel—A New Look into This Issue at Narrow Groove. *Metals* **2021**, *11*, 904. [CrossRef]

14. Schaupp, T.; Rhode, M.; Yahyaoui, H.; Kannengiesser, T. Influence of heat control on hydrogen distribution in high-strength multi-layer welds with narrow groove. *Weld. World* **2018**, *63*, 607–616. [CrossRef]

15. Qu, J.; Feng, M.; An, T.; Bi, Z.; Du, J.; Yang, F.; Zheng, S. Hydrogen-Assisted Crack Growth in the Heat-Affected Zone of X80 Steels during in Situ Hydrogen Charging. *Materials* **2019**, *12*, 2575. [CrossRef]

16. Magnusson, H.; Frisk, K. Diffusion, Permeation and Solubility of Hydrogen in Copper. *J. Phase Equilibria Diffus.* **2017**, *38*, 65–69. [CrossRef]

17. Peñalva, I.; Alberro, G.; Legarda, F.; Esteban, G.A.; Riccardi, B. Interaction of Copper Alloys with Hydrogen. In *Copper Alloys-Early Applications and Current Performance-Enhancing Processes*; Collini, L., Ed.; IntechOpen: London, UK, 2012. [CrossRef]

18. Marchi, C.S.; Somerday, B.P. *Technical Reference on Hydrogen Compatibility of Materials*; SAND2012-7321; Sandia National Laboratories: Livermore, CA, USA, 2012.

19. Kannengiesser, T.; Tiersch, N. Measurements of Diffusible Hydrogen Contents at Elevated Temperatures using Different Hot Extraction Techniques—An International Round Robin Test. *Weld. World* **2010**, *54*, R115–R122. [CrossRef]

20. Rhode, M.; Schaupp, T.; Muenster, C.; Mente, T.; Boellinghaus, T.; Kannengiesser, T. Hydrogen determination in welded specimens by carrier gas hot extraction—A review on the main parameters and their effects on hydrogen measurement. *Weld. World* **2019**, *63*, 511–526. [CrossRef]

21. *ISO 3690:2018-07*; Welding and Allied Processes-Determination of Hydrogen Content in Arc Weld Metal. International Organization for Standardization: Vernier, Geneva, Switzerland, 2018.

22. Mente, T.; Boellinghaus, T.; Schmitz-Niederau, M. Heat treatment Effects on The Reduction of Hydrogen in Multi-Layer High-Strength Weld Joints. *Weld. World* **2012**, *56*, 26–36. [CrossRef]

23. Nevasmaa, P. Prevention of Weld Metal Hydrogen Cracking in High-Strength Multipass Welds. *Weld. World* **2004**, *48*, 2–18. [CrossRef]

24. Padhy, G.K.; Komizo, Y. Diffusible Hydrogen in Steel Weldments: A Status Review. *Trans. JWRI* **2013**, *42*, 39–62.

25. Świerczyńska, A.; Fydrych, D.; Łabanowski, J. The Effect of Welding Conditions on Diffusible Hydrogen Content in Deposited Metal. *Solid State Phenom.* **2011**, *183*, 193–200. [CrossRef]

26. Kannengiesser, T.; Lausch, T. Diffusible Hydrogen Content Depending on Welding and Cooling Parameters. *Weld. World* **2012**, *56*, 26–33. [CrossRef]

27. Padhy, G.K.; Ramasubbu, V.; Murugesan, N.; Remash, C.; Albert, S.K. Effect of preheat and post-heating on diffusible hydrogen content of welds. *Sci. Technol. Weld. Join.* **2012**, *17*, 408–413. [CrossRef]

28. *ISO 24373:2018-11*; Welding Consumables–Solid Wires and Rods for Fusion Welding of Copper and Copper Alloys-Classification. International Organization for Standardization: Vernier, Geneva, Switzerland, 2018. [CrossRef]

29. *EN 10027-2:2015*; Designation Systems for Steels–Part 2: Numerical System. CEN-CENELEC: Brussels, Belgium, 2015.

30. *ISO 17639:2022-01*; Destructive Tests on Welds in Metallic Materials-Macroscopic and Microscopic Examination of Welds. International Organization for Standardization: Vernier, Geneva, Switzerland, 2022.

31. Lee, S.J.; Sharma, A.; Jung, D.H.; Jung, J.P. Influence of Arc Brazing Parameters on Microstructure and Joint Properties of Electro-Galvanized Steel. *Metals* **2019**, *9*, 1006. [CrossRef]

32. Savage, W.F.; Nippes, E.F.; Stanton, R.P. Intergranular Attack of Steel by Molten Copper. *Weld. J.* **1978**, *57*, 9–16.

33. Chen, S.; Yu, X.; Huang, J.; Yang, J.; Lin, S. Interfacial ferrite band formation to suppress intergranular liquid copper penetration of solid steel. *J. Alloys Compd.* **2019**, *773*, 719–729. [CrossRef]